

N 7 2 - 2 8 8 7 1 .

MSC-06755

NASA TECHNICAL MEMORANDUM

NASA TM X-58089
March 1972



CASE FILE
COPY

INFLIGHT DYNAMICS TESTING OF THE APOLLO SPACECRAFT

NATIONAL AERONAUTICS AND SPACE ADMINISTRATION

MANNED SPACECRAFT CENTER

HOUSTON, TEXAS 77058

1. Report No.		2. Government Accession No.		3. Recipient's Catalog No.	
4. Title and Subtitle INFLIGHT DYNAMICS TESTING OF THE APOLLO SPACECRAFT				5. Report Date March 1972	
				6. Performing Organization Code	
7. Author(s) William H. Peters and Bernard Marcantel, MSC				8. Performing Organization Report No.	
9. Performing Organization Name and Address Manned Spacecraft Center Houston, Texas 77058				10. Work Unit No. 914-50-30-02-72	
				11. Contract or Grant No.	
12. Sponsoring Agency Name and Address National Aeronautics and Space Administration Washington, D. C. 20546				13. Type of Report and Period Covered Technical Memorandum	
				14. Sponsoring Agency Code	
15. Supplementary Notes The MSC Director waived the use of the International System of Units (SI) for this Technical Memorandum, because in his judgment, the use of SI units would impair the usefulness of the report or result in excessive cost.					
16. Abstract Response of the Apollo command module, service module, and lunar module airframes while in a docked configuration in the flight environment was measured in a frequency band encompassing the first two bending modes. Transfer characteristics from thrust-application point to control-system sensor were examined. The frequency and the stability margins of the first two predominant structural resonances were verified by the test. This report describes the flight test that was performed and the postflight data analysis.					
17. Key Words (Suggested by Author(s)) • Apollo Spacecraft • Structural Dynamics • Inflight Test • Frequency Response • Stability Margin				18. Distribution Statement	
19. Security Classif. (of this report) None		20. Security Classif. (of this page) None		21. No. of Pages 37	22. Price

CONTENTS

Section	Page
SUMMARY	1
INTRODUCTION	1
TEST DESCRIPTION	2
JUSTIFICATION FOR INFLIGHT DYNAMICS TESTING	3
MISSION AND PROGRAM IMPACT	5
Flight Test Procedures	5
Trade-Off Regarding Risk	6
TEST PREPARATION	7
Preflight Analysis and Simulation	7
Postflight Analysis Plan	8
TEST DATA ANALYSIS	11
TEST RESULTS	13
CONCLUSIONS	14
REFERENCES	14

FIGURES

Figure		Page
1	Stroking-test excitation function	15
2	Relationship of the structural ground test and the stroking test in flight to the control-system developmental process	16
3	Docking-tunnel load response to the stroking test of the CSM/LM digital autopilot	17
4	Time response for the SPS engine pitch gimbal position	18
5	Time response for the SPS engine pitch actuator command	19
6	Time response for the pitch body rates	20
7	Frequency spectrum for the SPS engine pitch actuator command	21
8	Frequency spectrum for the SPS engine pitch gimbal position	22
9	Frequency spectrum for the pitch body rates	23
10	Time response for the roll body rates	24
11	Time response for the yaw body rates	25
12	Frequency response for the SPS engine pitch actuator	
	(a) Amplitude ratio	26
	(b) Phase angle	27
13	Postflight airframe transfer function	
	(a) Amplitude ratio	28
	(b) Phase angle	29
14	Total-system transfer function	
	(a) Amplitude ratio	30
	(b) Phase angle	31
15	Preflight total-system transfer function	
	(a) Amplitude ratio	32
	(b) Phase angle	33

INFLIGHT DYNAMICS TESTING OF THE APOLLO SPACECRAFT

By William H. Peters and Bernard Marcantel
Manned Spacecraft Center

SUMMARY

The Apollo lunar-landing missions require a large velocity-change maneuver for lunar orbit insertion while the command-service module is docked to the lunar module. Design of the autopilot for this maneuver required special care to avoid inducing an instability in the primary structural resonances. Several important dynamic effects could not be thoroughly investigated in the ground testing because they involved the engine-thrust forces of the service propulsion system. Therefore, potential sources of error in the analytical predictions of the inflight dynamic response of the predominant structural resonances could be evaluated only by means of inflight dynamics testing. This report describes the inflight dynamics test performed on the Apollo 9 mission. The stability of the attitude control system, for the docked configuration during main engine thrusting, was demonstrated by analysis of data from the flight test. These data yielded airframe transfer function response information in the form of bode plots. Pronounced effects of dynamic coupling between the thrust-vector-control system and the rest of the spacecraft were not evident in the flight data.

INTRODUCTION

The Apollo lunar-landing missions require a large velocity-change maneuver with the command-service module (CSM) and the lunar module (LM) joined at the docking tunnel. This maneuver is performed by thrusting with the main rocket engine of the service propulsion system (SPS). The SPS engine is attached to the service module airframe by means of a gimbal ring and two electromechanical gimbal actuators. Spacecraft attitude is maintained by controlling the SPS engine gimbal angles with the actuators.

Design of the autopilot for use during the long lunar-orbit-insertion burn required special care to avoid inducing an instability in the primary structural resonances. The preflight predictions of the inflight dynamic response of the CSM/LM airframe, coupled with the SPS engine actuation dynamics, were accomplished only through an analytical extrapolation of the structural response obtained by performing modal tests of the docked configuration on the ground.

Several important dynamic effects could not be thoroughly investigated in the ground testing, because they involved the engine-thrust forces. Therefore, it appeared that potential sources of error in the analytical predictions of the inflight dynamic

response of the predominant structural resonances could be evaluated only by means of inflight dynamics testing. The inflight dynamics test described in this report was called the "stroking" test because of the manner in which the excitation was applied.

This report describes the stroking test performed on the Apollo 9 mission, provides a justification for the test, describes test procedures and criteria, gives an account of the preflight analysis that was performed, describes the postflight analysis plan, and presents the results of the detailed postflight analysis.

TEST DESCRIPTION

The fundamental concept associated with the stroking test is "frequency response." The frequency response of a plant (or process) to which control inputs must be applied is perhaps the most descriptive characteristic that can be measured. This fact is particularly true if closed-loop control is required and if conditions are such that sustained oscillations can occur. If this situation exists, dynamic compensation must be designed, and information about the frequency-response characteristics of the plant (or process) to be controlled becomes essential.

A frequency-response test is normally thought of in terms of a long, drawn-out process, where sinusoidal excitations are applied on a single-frequency basis for numerous frequencies. If the plant is assumed to be a linear system, the principle of superposition may be applied to show that it is unnecessary to apply excitation inputs on an individual basis. An additional concern of frequency-response testing is the belief that steady-state conditions must be achieved after application of each test input (sinusoidal excitation). This statement is true in single-frequency testing because the normal method of data reduction does not account for the fact that the dynamic state of the device is "at rest" when the excitation begins.

The following were the basic principles of the stroking test.

1. Excitation was assumed to have been applied for long times before and after the actual physical application of the test signal.
2. The excitation was assumed to be composed of an infinite number of individual test inputs, all of which were sinusoidal and were applied simultaneously.
3. The amplitudes and phase relationships of the test inputs were such that the net result (a) was zero up to the point in time at which the actual physical stroking began, (b) was exactly equal to the stroking signal during the interval of signal application, and (c) was again zero for all time thereafter.

Choosing the amplitudes and phase relationships of the individual test inputs in this manner permitted the use of an extremely short total excitation time (7.3 seconds for the Apollo 9 test).

The Apollo 9 test was performed by commanding the SPS engine pitch gimbal actuator at a constant rate for a short period of time, reversing the polarity of the drive command for another period of time, and repeating the process to form a series of

ramp inputs. The excitation signal for the actuator command is shown in figure 1. It should be noted that the excitation was designed to be symmetrical so that no residual angular velocity would remain after the test. The excitation signal was generated by a subroutine in the command module computer, which is independent of structural response and normal controller action. The signal was then summed with the normal controller commands to the SPS engine actuator. This forcing function was designed by an iterative analytic process that yielded a nearly flat power-density spectrum between 1.0 and 3.0 hertz, with very little energy at frequencies outside this band.

The control system would treat the test input as a disturbance and thereby generate commands to cancel the stroker input. However, the controller for the Apollo 9 configuration was designed to provide large attenuations at frequencies above 0.1 hertz, and the net result was that the engine angle command was nearly identical to the stroking command. Even if the actual engine position-time history had differed significantly from the stroking command (because of a guidance input, for example), the test would still have been valid. The SPS engine position data were telemetered; therefore, the true excitation of the CSM/LM airframe would have been known. The actual format of the required excitation signal was arbitrary as long as certain constraints were met. The constraints were (1) sufficient excitation of the significant elastic modes of interest and (2) acceptable structural loads and crew comfort. The excitation function of figure 1 was shown to meet these criteria with the control and guidance loops functioning in a closed-loop simulation.

JUSTIFICATION FOR INFLIGHT DYNAMICS TESTING

The objectives in the original request for the inflight dynamics testing were more ambitious at the time of the request than at the time of the actual testing because it was hoped that triaxial, linear accelerometers could be added and that telemetry would be available from the docked LM. As a result of tight schedules, the high demand for telemetry channels, high costs for the addition of measurements, and so forth, the additional telemetry was disallowed. Furthermore, to obtain telemetry from the LM during the SPS burn performed while the CSM and LM are docked would add a constraint on the mission time line (i. e., result in a requirement for the crew to power up the LM sooner than would normally be done).

Elimination of the telemetry left only the CSM rate-gyro information available as structural-response data and eliminated one of the original prime justifications for the testing — that of providing data to the structural analyst for calibration of the mathematical models used in the generation of bending-mode shape information. In other words, bending-mode shape information could not be obtained from the rate-gyro measurement alone. However, the dynamic gain characteristic of the structural-response transfer function over a frequency band that encompasses the first two bending modes could be obtained. In addition, phase-shift information could also be obtained. These data were precisely the information needed for an end-to-end flight verification of the structural dynamics model coupled with the control system (under a thrusting environment). This information would provide a measure of the attitude-control-loop stability margin at the predominant structural resonances. (The stability margins of all the structural resonances could not be verified without additional stroking tests that would accentuate other frequency bands.) Hence, the primary objective of the testing

was to measure the response of the CSM/LM airframe (while the airframe was dynamically coupled to the SPS engine actuation system) in a frequency band encompassing the first two structural bending modes. ("Response," as used in this report, implies total time-domain response at a particular structural point and not total time-domain response at all structural points.) This measurement would provide a measure of the stability margins on these two modes because the frequency response of the controller at these frequencies was well known.

It should be stressed that the inflight dynamic response would be known (before execution of the stroking test) only through analytical extrapolation of the structural-response data obtained by performing modal tests of the docked configuration on the ground. Dynamic effects that were treated analytically beyond the structural ground testing or that were not treated in the analytical processes because of value judgments are as follows.

1. The suspension system causes small dynamic forces as a result of interaction with the suspension mode and as a result of suspension-system damping forces. Because of sizable separation in frequency between the suspension mode and the first structural mode, these forces should be small and probably were accounted for with sufficient accuracy.

2. Dynamic forces from sloshing propellants couple with the structural resonances. The characteristic frequencies of the fundamental propellant-sloshing modes during the ground testing were approximately twice those expected in flight (i. e., for the LM docked with the CSM). This effect, which is difficult to account for analytically in an exact manner, was not entered in the analysis as a result of a value judgment that ruled in favor of accepting the uncertainty rather than spending the additional effort and time required to compensate for this effect in the analysis.

3. The effects of the coupling paths for energy flow from the SPS engine actuator motors into the structural resonances are of two types. The first type is the first-order effects that are believed to be properly treated in the analytical models. These effects are the engine inertial torques, caused by addition of an actuator-length degree of freedom, which produce dynamics referred to by previous authors as "tail wags dog." The second type, believed to be of second-order importance, is not treated by the existing analytical models. This effect included a forcing of the bending modes through the compliance of the actuator attach points and a coupling with the torsional modes as a result of actuator-motor reaction forces.

4. It is possible for the combined airframe and rocket engine gimbal-actuation dynamics, when coupled through the thrust force, to be an unstable plant, even without any attitude-control-loop feedbacks. This is due to a coupling phenomenon that will be termed "dog wags tail." This coupling results from phase lags between application of inertial torques to the engine (by airframe oscillations) and resulting engine motions relative to airframe coordinates that differ from the 0° or 180° phase relationships that exist in normal modes of spring-mass systems. Preflight analysis had predicted that this type of instability could exist in the Apollo vehicle for a severe combination of tolerances on vehicle data.

The logic flow for integrating structural dynamics data into the overall powered-flight control-system design and developmental process is shown in figure 2. It should

be noted that the inflight stroking test fills a basic need in the control-system design verification. Additional discussion pertinent to the overall justification for the test appears in the section of this report entitled "Trade-Off Regarding Risk."

MISSION AND PROGRAM IMPACT

The primary mission requirement for performance of the stroking test was a relatively long SPS engine burn while the CSM and LM were in the docked configuration. This burn resulted in a small mission planning impact for the once-planned Apollo 207/208 mission; but, fortunately, when the mission was changed to a Saturn V booster configuration, the plan contained two long out-of-plane SPS engine burns. This plan provided the ideal situation for performance of the stroking test. The plan also allowed ample time for an initial test at reduced amplitude, for real-time safety evaluation, for test amplitude change, and for one final test, without significant effect on the crew time line. The detailed test procedures and the inherent risks involved, both with and without the stroking test, are discussed in the following sections.

Flight Test Procedures

The stroking test was performed in a completely automatic mode, with the exception that the test was manually enabled by execution of verb 68 on the display and keyboard in the command module. If this verb had been executed at any time other than during an SPS burn under digital autopilot control, the operator-error alarm light would have been activated, and control would have been returned to the program previously executed. If the stroking test had been enabled after thrust initiation time T_{ig} (but before $T_{ig} + 10$ seconds), the excitation would have begun at $T_{ig} + 10$ seconds. The test was enabled after $T_{ig} + 10$ seconds, and the excitation began immediately.

The excitation terminated automatically 7.3 seconds after it began, but the requirement for test data stipulated that the burn must continue for several seconds beyond that point. The exact amount of burn time required beyond the end of the excitation for the test is a function of the following parameters.

1. Excitation amplitude
2. Telemetry threshold
3. Structural-response data characteristics
4. Information-quality requirements

Because the information-quality requirements are somewhat subjective in nature and because structural-response data characteristics were not well known, the exact time requirement for data to be obtained was not known. Once models were assumed for the first three items, however, it was shown that the quality of the information that could be derived from the data improved, to a certain point, with the length of the data-gathering interval and then degraded for longer intervals. Analysis showed that a burn

time between 20 and 30 seconds beyond termination of the excitation for the test was required for the Apollo 9 mission. The detailed test objective for the Apollo 9 mission stated that the test should be initiated at least 34 seconds before the end of the burn; this requirement assured ample time for data gathering before thrust termination.

The flight procedures established performance of the stroking test in two basic parts. The first time the test excitation was activated, it produced the desired waveform, but all amplitudes were scaled at 40 percent of the required nominal amplitude. The crew and ground controllers then judged that a full-amplitude run was safe, a single constant in the erasable memory (ESTROKER at location 3013) was changed from octal digit 00002 to 00005, and the test was repeated on the next SPS engine burn. As another possible flight-procedure variant, it would have been acceptable to perform both the 40-percent-amplitude and the full-amplitude passes in the same burn, provided that at least 40 seconds had been allowed to elapse between initiation of the first and the final passes.

If a premature termination of the excitation had been desired, a forced computer restart could have been employed by using verb 69. An alternate test abort procedure would have been to switch to the backup control system.

Trade-Off Regarding Risk

The effect of the stroking test on mission planning and crew activity was quite small. Therefore, the remaining consideration was the risk involved as a result of not performing the test, as opposed to the risk involved in performing the test.

It should be recognized that a certain element of risk existed in that the attitude control system would be unstable when the SPS engine was initially ignited for the first burn on the Apollo 9 mission. Every reasonable effort had been made to assure that this situation would not occur, but still a small probability existed that something may have been erroneously judged to be insignificant or not even considered in the analytical process. Without the stroking test, this small probability that an instability would occur would have been increased with burn time on the Apollo 9 and each succeeding mission.

Now that the stroking test has been performed and reasonable stability margins have been validated, the probability of a powered-flight control-system instability for future flights is essentially zero. Furthermore, it should be emphasized that performance of the test did not affect the probability of instability on the Apollo 9 mission, if linear response is assumed. Hence, performance of the stroking test "traded off" the small probability of a future powered-flight instability for a small probability of crew discomfort or structural damage (or both) as a result of the stroking test.

It was impractical to compute realistic probability data for comparative purposes. However, with extensive preflight analysis and testing (as discussed in the following sections) and with a prudent flight test procedure (as described previously), the risk associated with test performance was judged to be acceptable.

TEST PREPARATION

The section entitled "Preflight Analysis and Simulation" briefly summarizes the work that was performed in design of the test excitation signal, demonstration of the validity of the analytic technique, investigation of data requirements, software verification for the stroking test, structural loads computations, and hardware tests. A post-flight analysis plan is also presented.

Preflight Analysis and Simulation

The final signal design evolved (fig. 1) after the decision was made to use a nearly flat power-density spectrum and after the software constraints were taken into account. A design study was then performed that demonstrated the effectiveness of the analytic techniques to be used. The effectiveness was determined from operation on the simulated vehicle time response to generate a transfer function from the time-domain data. The exercise was repeated for assumed data-gathering intervals of 27 and 57 seconds. When both noise caused by nonzero initial conditions and imperfections in data retrieval were assumed to be nonexistent, the amplitude ratio error for 57 seconds of data was 1.5 decibels, while that for 27 seconds of data was 5.5 decibels.

The effects of telemetry quantization and telemetry-channel saturation on reconstruction of the airframe transfer function were investigated. The telemetered data were transmitted by means of an 8-bit word. As a result of this method of transmission, the dynamic range of the measurement channel was broken into 256 parts. The dynamic range of the rate information would be either 10.0 or 2.0 deg/sec, depending on whether the ± 5 - or the ± 1 -deg/sec scale on the flight director attitude indicator was chosen by the astronaut. This range gives rate data quantization in increments of 0.0376 and 0.0075 deg/sec, respectively. Hence, less high-frequency quantization noise is present if the smaller scale is chosen, but then a small risk exists that the rates may exceed 1.0 deg/sec during the test, and information may be lost. The effects of these two data coarseness levels and the results for "clipping" as much as 20 percent at peak amplitudes (i. e., running the gyro response data through a limiter with the limit value set at 80 percent of the peak response) were examined.

The essential conclusions of the study were that neither the data quantization nor channel saturation would seriously degrade construction of the amplitude ratio by more than 2.5 decibels at the resonant peaks of the first two structural bending modes. The phase data were affected very little by the 0.0075-deg/sec quantization (at the ± 1 -deg/sec scale) or by the 20-percent data clipping, but the data were degraded significantly by the 0.0376-deg/sec quantization (at the ± 5 -deg/sec scale). These results imply that the ± 1 -deg/sec scale should be used.

The effects of sensor dynamics were examined and found to be negligible; however, a hardware change for block II spacecraft caused additional distortion. This change and the resultant distortion of the data are discussed in the section entitled "Test Data Analysis."

Time-response data from the simulator at the spacecraft contractor's facilities described in reference 1 are presented in figure 3. This simulation used a flight

hardware computer, a flight program (SUNDISK 282), a hardware SPS engine actuator, coupling data units, and a display and keyboard. Eleven bending modes were used in what is thought to be a reasonably accurate flexible-body dynamics model, and a reasonably accurate docking tunnel loads computation was used. The stroking test was initiated through the display and keyboard in the command module by means of verb 68. The peak torsional loads indicated were approximately one-third the expected tolerable level. (Later simulations using structural data from the structural ground test indicated even greater margins.) The stroking-test forces were simulated during the structural ground test, which also showed that structural loads resulting from the nominal stroking amplitude were well within tolerable levels.

Postflight Analysis Plan

The section entitled "Test Description" discusses the background theory related to the stroking test in general terms. References 2 to 4 provide more detailed information on some of the broader aspects. The output of a linear system $y(t)$ can be obtained by summing all past unit impulse responses $h(t - \tau)$, weighted by the value of the input function at time $t = \tau$; that is, $x(\tau)$. Stated symbolically

$$y(t) = \int_{-\infty}^t x(\tau)h(t - \tau)d\tau \quad (1)$$

In the limit, as $t \rightarrow \infty$, the Fourier transform of $y(t)$ can be expressed as the product of the Fourier transforms of $x(t)$ and $h(t)$; that is, if

$$\left. \begin{aligned} F[y(t)] &= Y(j\omega) \\ F[x(t)] &= X(j\omega) \\ F[h(t)] &= H(j\omega) \end{aligned} \right\} \quad (2)$$

then

$$Y(j\omega) = X(j\omega)H(j\omega) \quad (3)$$

If $x(t)$ is the telemetered stroking function (excitation) and $y(t)$ is the telemetered vehicle-response function, then, by processing these time-response functions to obtain their Fourier transforms $X(j\omega)$ and $Y(j\omega)$, respectively)

$$H(j\omega) = \frac{Y(j\omega)}{X(j\omega)} \quad (4)$$

Equation (4) is a theoretical result that is not completely attainable in practice for the following reasons.

1. Exact analytical expressions for the two time functions are not available.
2. Telemetry thresholds and other effects add noise to the accumulated data.
3. Numerical techniques for computing the Fourier transforms have limitations in the dynamic range and accuracy problems because of time quantization of the data.

As a result of these constraints, equation (4) will be valid only for certain intervals of ω (i. e., those frequency intervals in which the response data are reasonably representative of the true system response to the input).

For the Apollo 9 stroking test, the excitation had been designed to provide a large amount of excitation in the range between 1.0 and 3.0 hertz and little elsewhere. Hence, for those characteristic dynamics in this frequency band that had significant contributions to the measured response, equation (4) was valid. The process had been demonstrated by using the response of an analytical model of the Apollo spacecraft, as discussed in the section entitled "Preflight Analysis and Simulation."

The original postflight data-reduction plan is listed as follows. However, all these steps were not actually performed on the data as a result of poor data quality; further elaboration on this subject appears in the section of this report entitled "Test Data Analysis."

1. Obtain the following time-history measurements from telemetry data: pitch, yaw, and roll body rates; pitch differential current; SPS engine pitch and yaw gimbal position commands; SPS engine pitch and yaw gimbal positions; yaw channel guidance command; and roll control torques from the reaction control system.

2. Obtain Fourier transforms for each time function, assuming the values of the functions to be identically zero for all time preceding initiation of the excitation and to be zero for all time after approximately 40 seconds from test initiation.

3. Compute amplitude-ratio and phase-shift information as a function of frequency for the following transfer functions.

- a. The pitch body rate per pitch gimbal position command
- b. The yaw body rate per pitch gimbal position command
- c. The roll body rate per pitch gimbal position command
- d. The SPS engine yaw gimbal position per pitch gimbal position
- e. The pitch body rate per SPS engine pitch gimbal position
- f. The SPS engine pitch gimbal position per pitch position command

4. Construct power-density spectrum plots for the pitch differential current, the roll control torques from the reaction control system, and the yaw channel guidance commands.

5. Compare data from item 3a with the analytically predicted response by using structural data from the ground test. Differences in these data can be used to establish new control-system stability margins. If the differences are small, then a high probability exists that the analytical models treat all significant dynamic coupling effects with sufficient fidelity and depth. If the differences are large, then either the analytical models are inadequate or the data quality (and quantity) is not sufficient to provide conclusive answers.

6. Items 3b and 3c represent the crosscoupling from pitch control into yaw and roll control through the structural dynamics. These items will be meaningful data only if yaw and roll excitation from other sources is small in the frequency band in which stroking occurs (as determined from item 4).

7. Item 3d, which is a measure of the net crosscoupling into yaw control, is expected to be small compared with item 6 because of large attenuation in the yaw control filter.

8. Item 3e may provide a calibration point with the structural data obtained in ground testing. If good agreement is obtained between the amplitude-ratio and phase-angle information of these data in comparison with those obtained from the ground testing, then a high probability exists that the potentially significant effects discussed earlier are of little consequence. However, a significant disagreement may mean simply that the "tail wags dog" effects are large. This assumption cannot be established exactly, but an attempt can be made to bring item 3e data into agreement with the ground test data by compensating for the effects as follows: (a) Constructing an analytical airframe model that can be forced by pitch differential current only through the resulting engine inertial forces. (b) Subtracting this time function from pitch body rate and recomputing item 3e. Good agreement after these manipulations would constitute additional verification of the analytical models used for control-system design.

9. Item 3f will yield the transfer function of the coupled actuator and provide information on the extent of the dynamic coupling of the actuator with the airframe through the effect of the energy flow from the thrust force into the structural resonances.

10. Item 4 provides information on potential obscuration of data, which is caused by inputs other than the intended excitation. Pitch-body-rate gyro response caused by yaw guidance commands and roll torques, for example, would be computed from an analytical model and compared with pitch body rate. If this exercise should indicate that pitch-body-rate data are significantly affected by these excitation sources, then an attempt would be made to compensate for these inputs by subtracting their estimated contributions.

TEST DATA ANALYSIS

The full-amplitude test signal was initiated at 25:18:34.48 mission-elapsed time, approximately 60 seconds after the start of the third SPS engine firing. Postflight analysis was performed from telemetered data on the body rates about the three spacecraft axes and from data on the SPS engine gimbal position in the pitch and yaw planes.

The time response of the telemetered engine gimbal position in the pitch plane is shown in figure 4. Symmetry of these data about a nonzero value was due to the gimbal being in a trimmed position, compensating for the center-of-gravity offset. The actuator-excitation signal was not directly available from telemetry data, but it was indirectly constructed from other test and analytical data. Previous analysis had indicated the actuator response had a delay of 0.120 second in response to the excitation signal. The portion of the pitch actuator command resulting from normal controller action was available from the computer down link every 2 seconds, and it was found to have only one change — 0.025° — during the entire stroking test. Consequently, the total actuator input signal was then known to be the same as the pure stroking signal with a starting time of 0.120 second before the SPS engine gimbal response. The actuator command so constructed is shown in figure 5.

Telemetered pitch-body-rate data resulting from the stroking test are shown in figure 6. The general shape of the response was as anticipated from preflight analysis, but the amplitude of the bending oscillations was approximately one-third smaller than expected. The nonsymmetrical appearance of these data is caused by the rigid body-rate response to the stroking test. The body rates were measured by stabilization and control-system rate gyros using the ± 1 -deg/sec scale. This information was telemetered by an 8-bit word quantizing the data into 256 parts of 0.0078 deg/sec. As a result of this quantization and the low response amplitudes, the useful information lasts only approximately 10 seconds beyond test initiation. The sampling rate of 100 samples per second was sufficient for the frequency band of interest and did not have a significant effect on the data.

The pitch-body-rate data (fig. 6) were taken directly from the rate display on the flight director attitude indicator on the Apollo 9 mission; therefore, the display-meter dynamics are reflected in the body-rate data received from the flight. The best-available calibration data for the flight director attitude indicator indicated approximately 3-decibel attenuation at the first two bending frequencies. Phase-angle data from calibration tests were not available. The frequency response of a linearized model derived from diagrams obtained from the manufacturer matched the amplitude ratio of the calibration data from the flight director attitude indicator. The frequency response of this linear model also indicated approximately 30° of phase lag at 3.0 hertz. The flight director attitude indicator has a nonlinear static friction characteristic at small meter rates, which adds another unknown, but most likely significant, effect on the phase-angle information.

An investigation was performed to find a unique analytical solution for determining the original rate response before the flight director attitude indicator dynamics. Various possible techniques were considered, but it became evident that no unique closed-form solution to this problem existed. Efforts to obtain an iterative solution were

abandoned because the low response amplitudes, noisy data, and model complexity made further work unfeasible.

Frequency-domain analyses were performed by taking the Fourier transforms of the time response and manipulating these data to obtain bode plots. Special-purpose digital-computer programs were used in the data reduction. Fourier transforms of (1) the pitch actuator position command, (2) the pitch gimbal position, and (3) the CSM pitch body rate were computed. The frequency spectrum of the pitch actuator command (fig. 5) is shown in figure 7. As may be observed in that figure, any information outside the frequency band between 4.5 and 21 rad/sec would not be considered a valid response to the stroking signal. The frequency spectrum of the pitch gimbal position (fig. 4) is presented in figure 8. A comparison of figures 7 and 8 indicates loss of energy at the higher frequencies. This loss was due to filtering by the SPS engine actuator and its inertial load. The frequency spectrum of the telemetered pitch body rates (fig. 6) is shown in figure 9. The peaks at 17.29 and 19.50 rad/sec clearly define the first two bending resonance frequencies. The large energy content at the lower frequencies was primarily caused by propellant sloshing and rigid-body response to the stroking signal.

Telemetered roll-body-rate data are shown in figure 10. The roll body rates indicated were present before and after test signal initiation. A frequency analysis of the data indicated that the predominant energy content was at frequencies well below the 4.5-rad/sec minimum frequency of the test signal energy. These roll-body-rate oscillations were at 2.9 rad/sec, corresponding to the predicted frequency of SPS propellant sloshing. Another observation from figure 10 is evidence of one firing of the reaction control system roll jets.

Telemetered yaw-body-rate data are shown in figure 11. The observed yaw bending excitation began near the end of the test signal and shortly after the firing of the reaction control system roll jets. Because the roll jets that fired were in the yaw plane, this excitation is expected to be influenced considerably by the reaction control system jet firing. Because of the roll jet firing and the low pitch-plane excitation, no concrete conclusions were drawn regarding pitch-to-yaw coupling through the structure, even though a considerable amount of coupling was anticipated by the preflight analyses.

The primary goal of this analysis was to find the frequency response of the following transfer functions: (1) the SPS engine pitch gimbal position per pitch actuator position command (fig. 12), (2) the pitch body rates per SPS engine pitch gimbal position command (fig. 13), and (3) the pitch body rates per SPS engine pitch actuator position command (fig. 14). These transfer functions were obtained by forming the complex ratios of the Fourier transforms of the appropriate time functions on a point-by-point frequency basis. This procedure gives the desired transfer function amplitude ratio and phase angle (bode plots) as a function of frequency. Desired information such as predominant resonance frequencies and stability margins are readily obtained from these plots. The feasibility of this method of analysis was demonstrated in preflight studies.

The preflight analytically derived frequency-response data for a CSM/LM transfer function (with the CSM having a quarter-full propellant load) are shown in figure 15. This response is a pitch body rate per SPS engine pitch actuator command frequency response. Data from the modal ground tests were used in deriving this transfer function; hence, figure 15 represents the latest available preflight information, which is

used for comparison with the airframe frequency-response characteristics constructed from the flight test data (fig. 14) discussed in the following section.

TEST RESULTS

Frequency-response plots of the transfer functions for the SPS engine actuator with flight environment inertial loads (fig. 12), the CSM/LM airframe (fig. 13), and the total system (fig. 14) were constructed from the Fourier transforms of the telemetered data discussed in the previous section. The SPS engine pitch actuator frequency-response plots are shown in figure 12. Corresponding data derived from laboratory test data (ref. 5) are also shown in figure 12. The amplitude-ratio curves of the preflight and flight test data agreed very closely (fig. 12(a)). The phase lag of the actuator transfer function, as determined from the flight data, was 15° larger at 3.0 hertz, decreasing to a difference of zero at 1.0 hertz (fig. 12(b)). This close match of the flight test actuator response with the laboratory data gave confidence in the method used for constructing the actuator command function. Strong coupling between the actuator response and the structural dynamics would have produced much larger peaks and valleys in the amplitude-ratio curve if the dynamic inertial coupling between the engine mass and the remainder of the spacecraft had been significant. The frequency response of the CSM/LM airframe coupled with the actuator is shown in figure 14. The first two bending resonances are clearly defined at 17.25 and 19.41 rad/sec with peak amplitude ratios of -9 and -15 decibels. Compensating for attenuation of the flight director attitude indicator at these resonance peaks would result in values of -6 and -12 decibels. These values agree closely with the preflight predictions (fig. 15) of 17.37 and 18.99 rad/sec with peak amplitude ratios of -1.5 and -6.6 decibels.

The postflight phase-angle response (fig. 14(b)) lagged behind the preflight prediction (fig. 15(b)) by approximately 100° at the bending frequency. Compensating the flight data by 30° for the known (linear model) dynamics of the flight director attitude indicator and by 15° for the difference in the actuator phase-angle plots gives a remaining discrepancy of approximately 55° in phase-angle information. This difference probably results from static friction in the flight director attitude indicator, which produces phase lag at low amplitudes. However, the amplitude-response data have also demonstrated that accurate knowledge of phase-angle data is not required to guarantee the stability margin. When the controller gain of -12 decibels (stabilization and control system at 17 hertz) is combined with the maximum measured bending resonance gain of -6 decibels, the minimum gain margin (18 decibels) is obtained. This stability margin is more than adequate to absorb uncertainty in the controller electronics and errors in the flight test accuracy.

The transfer function of the CSM/LM airframe is given in figure 13. These data are acceptable for direct comparison with ground test results because the active engine dynamics are mostly excluded. Again, the phase information is expected to be of qualitative value only.

CONCLUSIONS

1. The inflight dynamics testing that was performed on the Apollo 9 mission has been described in detail.
2. Preflight analyses and tests were performed that demonstrated the soundness of the basic approach and the safety of the test.
3. The stability of the attitude control system (both primary and backup) for the service propulsion system velocity-change maneuver with the lunar module docked to the command-service module, fully coupled with the engine actuation system dynamics and the first two predominant structural resonances, has been demonstrated by flight data. The smallest stability margins were determined to be 18 decibels, not allowing for data uncertainty.
4. Pronounced dynamic coupling between the service module thrust-vector-control system and the rest of the spacecraft was not evident in the flight data.
5. The frequency of the first two structural resonances was verified.
6. The test amplitude was too low to permit accurate and sufficient data for more complete reduction of the inertial coupling effects of spacecraft engine-mount accelerations on engine-control dynamics, the inertial coupling effects of engine-control accelerations on spacecraft body dynamics, and the pitch and yaw coupling effects on the control-loop stability margin.

Manned Spacecraft Center

National Aeronautics and Space Administration

Houston, Texas, March 27, 1972

914-50-30-02-72

REFERENCES

1. Anon.: Apollo Digital Autopilot Hardware Verification Study Final Report. North American Rockwell Corp., Space Division, Rept. SD69-442, July 1969.
2. Lee, Y. W.: Statistical Theory of Communication. John Wiley & Sons, Inc., 1960.
3. Wiener, Norbert: The Fourier Integral and Certain of Its Applications. Dover Publications, Inc. (New York), 1933.
4. Truxal, John G.: Automatic Feedback Control System Synthesis. McGraw-Hill Book Co., Inc., 1955.
5. Jansen, J. A.: Engineering Analysis Report, Verification of MOD-2A SPS Gimbal Actuator for Automatic SCS Thrust-Vector Control and Manual Thrust-Vector Control for CSM 101. North American Rockwell Corp., Space Division, Rept. SD68-425, May 1968.

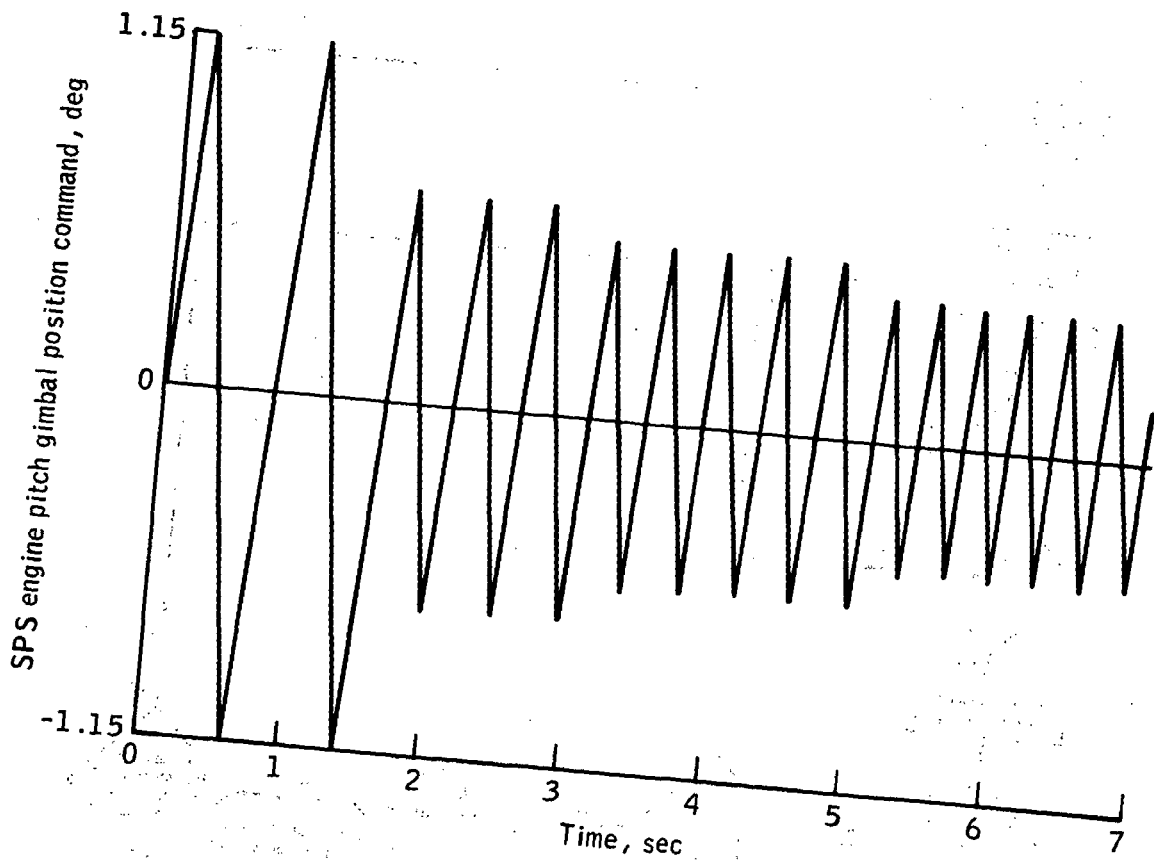


Figure 1. - Stroking-test excitation function.

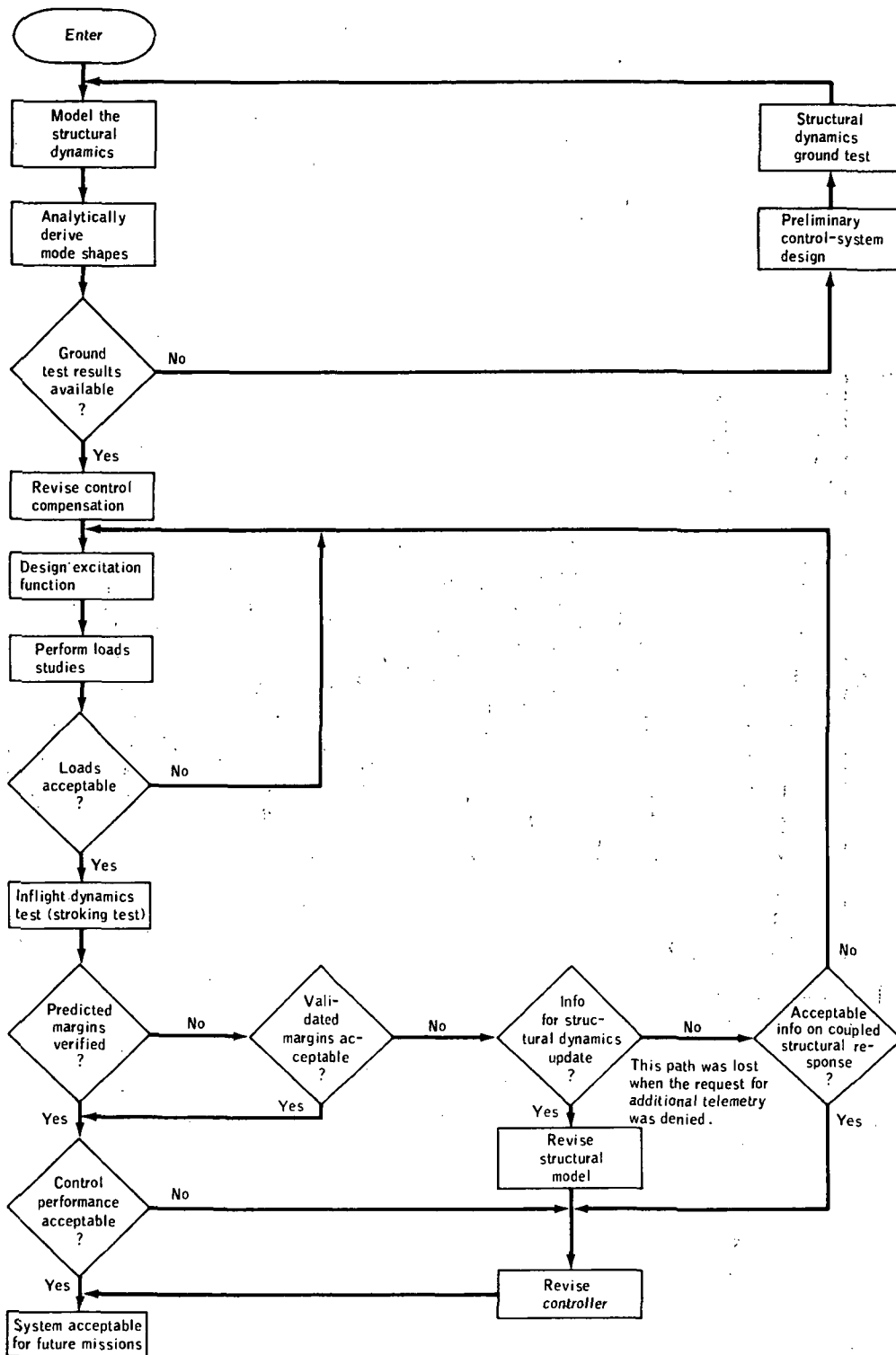


Figure 2. - Relationship of the structural ground test and the stroking test in flight to the control-system developmental process.

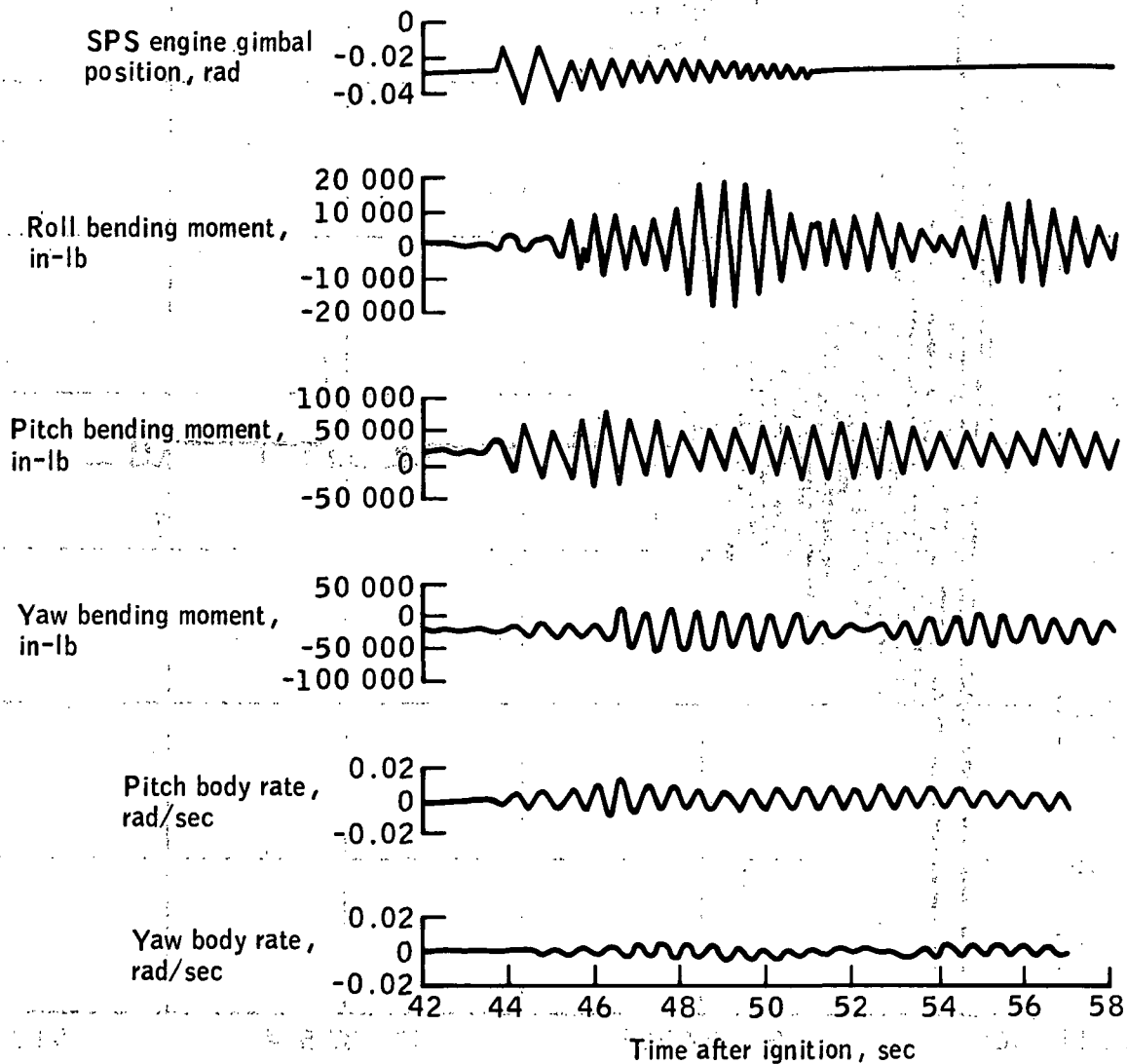


Figure 3. - Docking-tunnel load response to the stroking test of the CSM/LM digital autopilot.

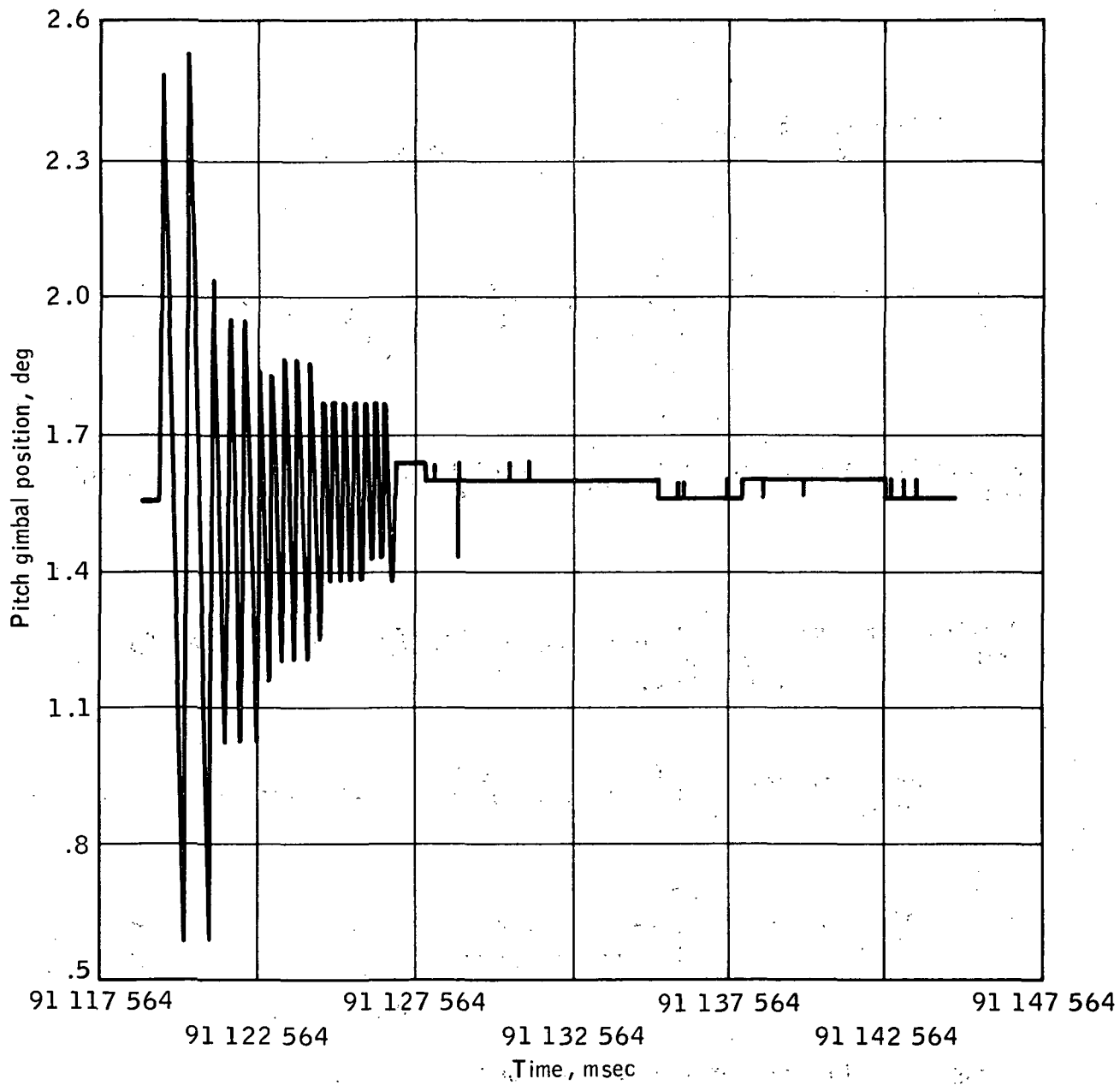


Figure 4. - Time response for the SPS engine pitch gimbal position.

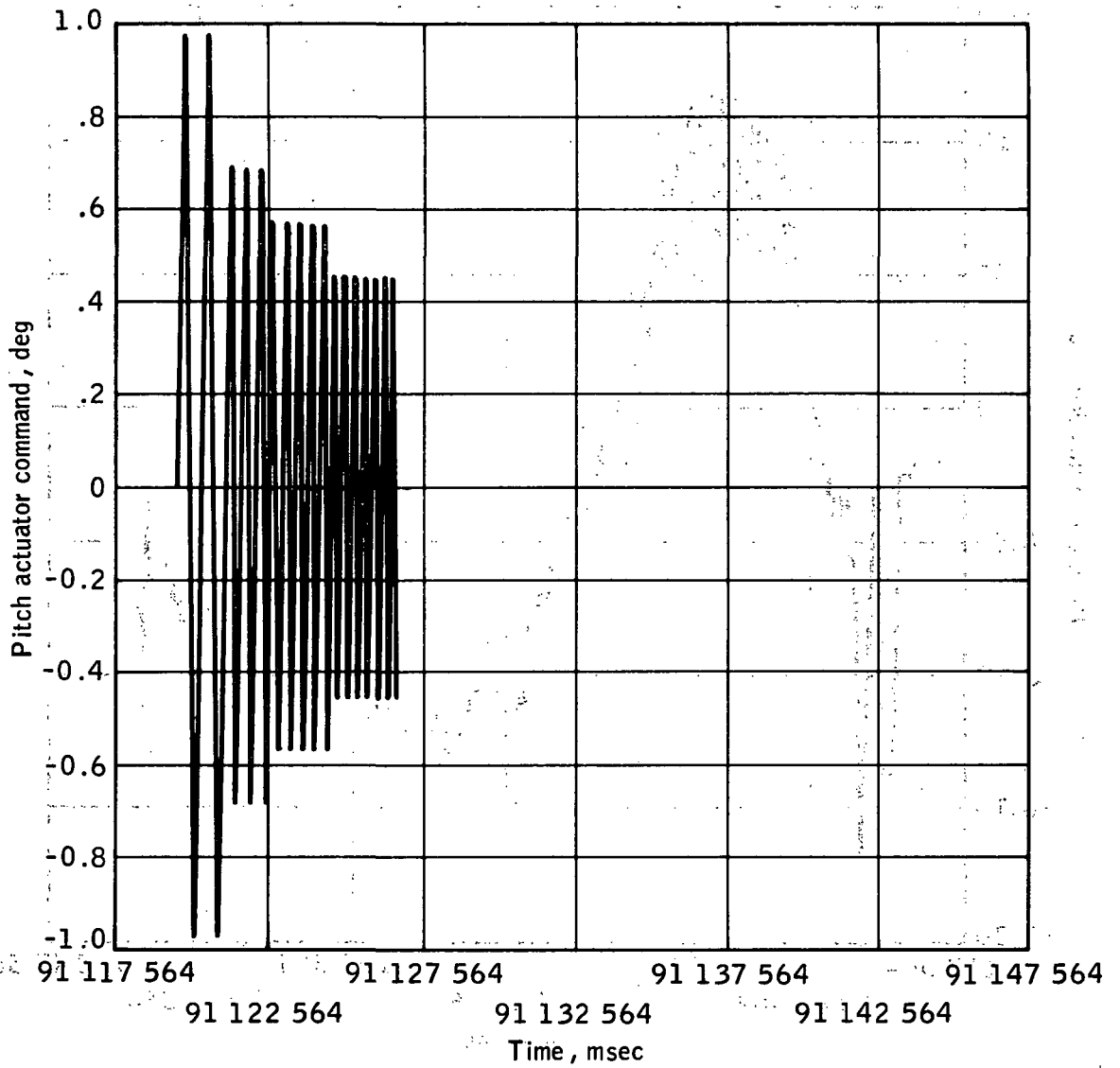


Figure 5. - Time response for the SPS engine pitch actuator command.

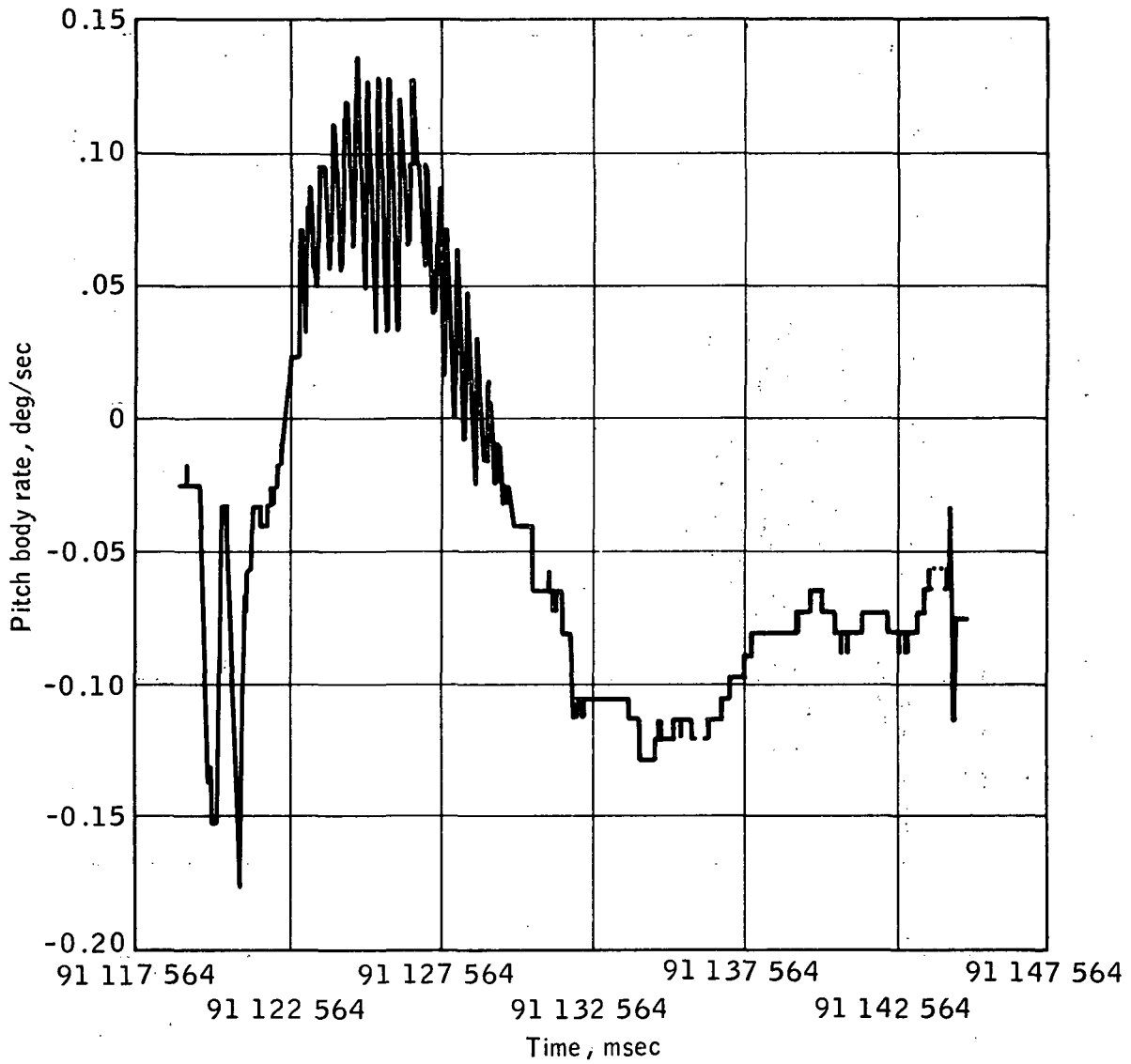


Figure 6. - Time response for the pitch body rates.

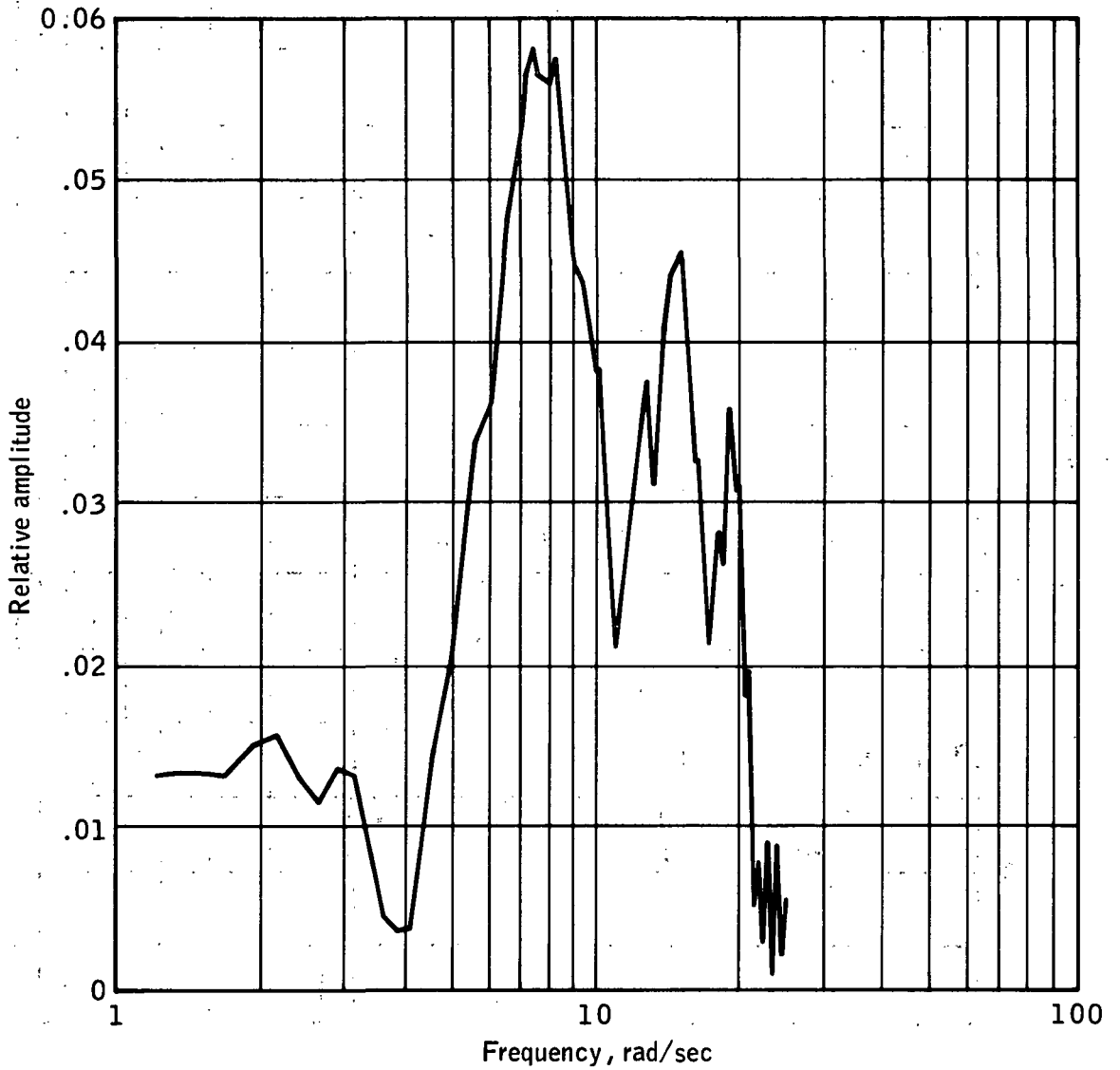


Figure 7. - Frequency spectrum for the SPS engine pitch actuator command.

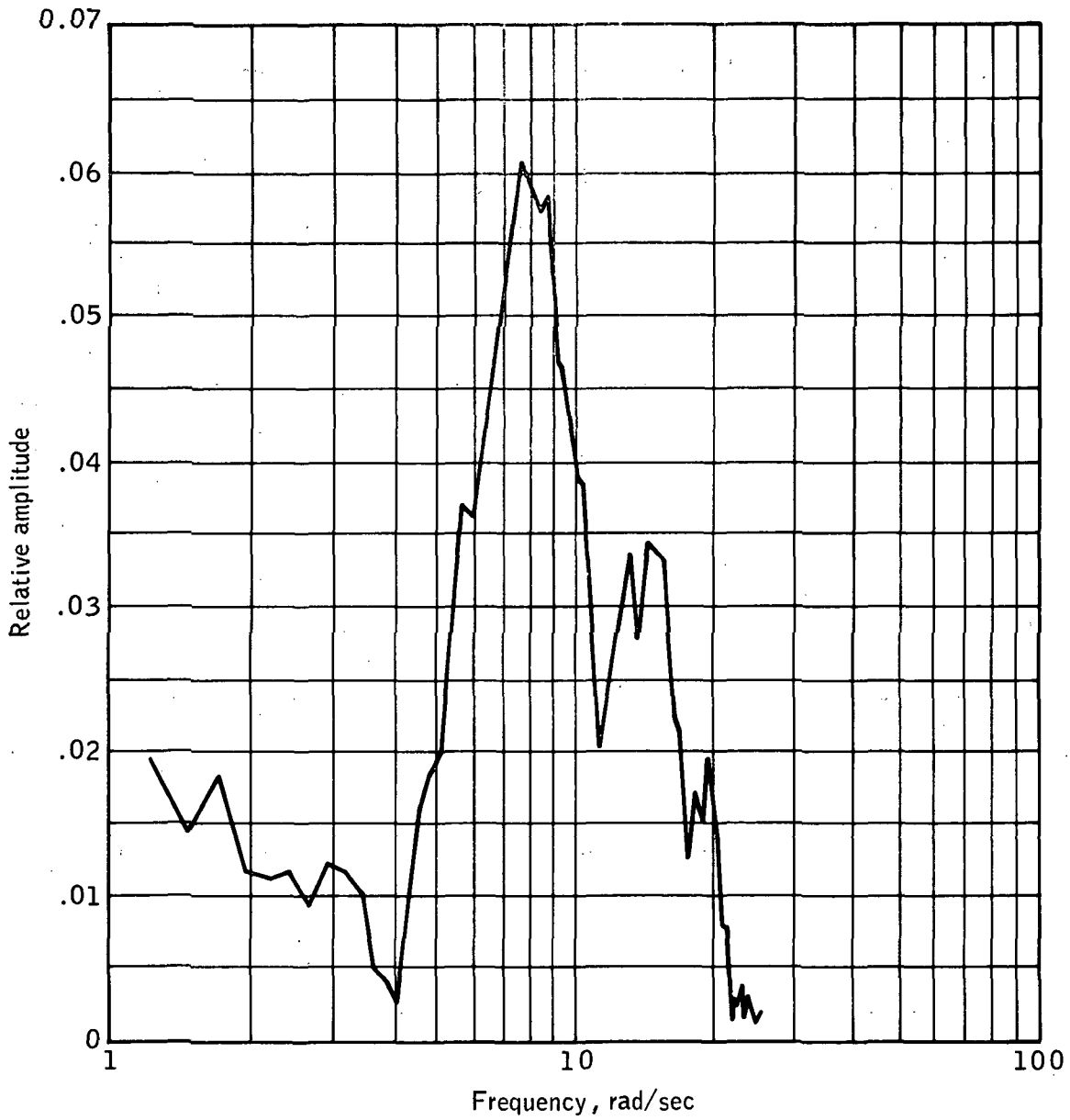


Figure 8. - Frequency spectrum for the SPS engine pitch gimbal position.

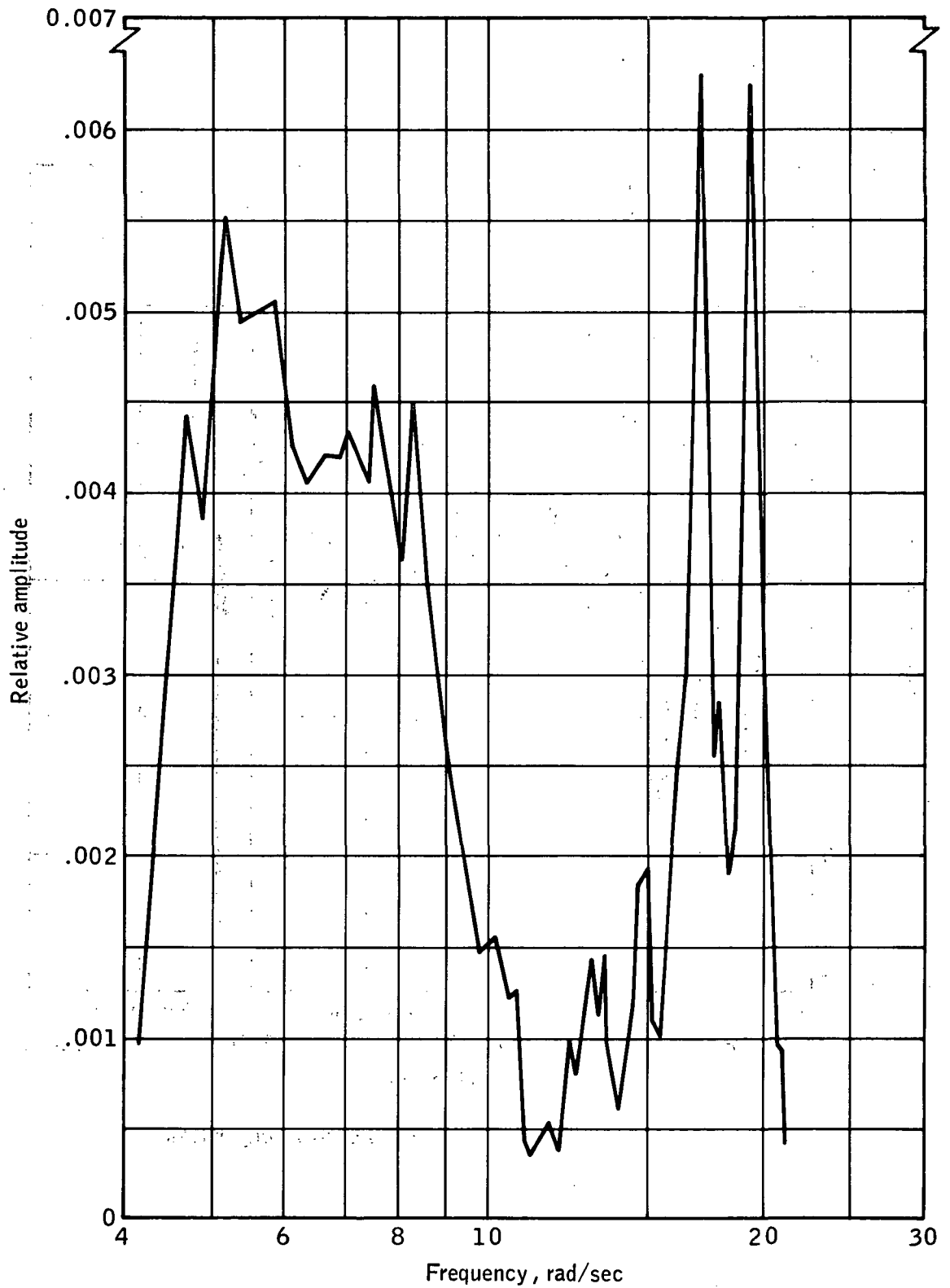


Figure 9. - Frequency spectrum for the pitch body rates.

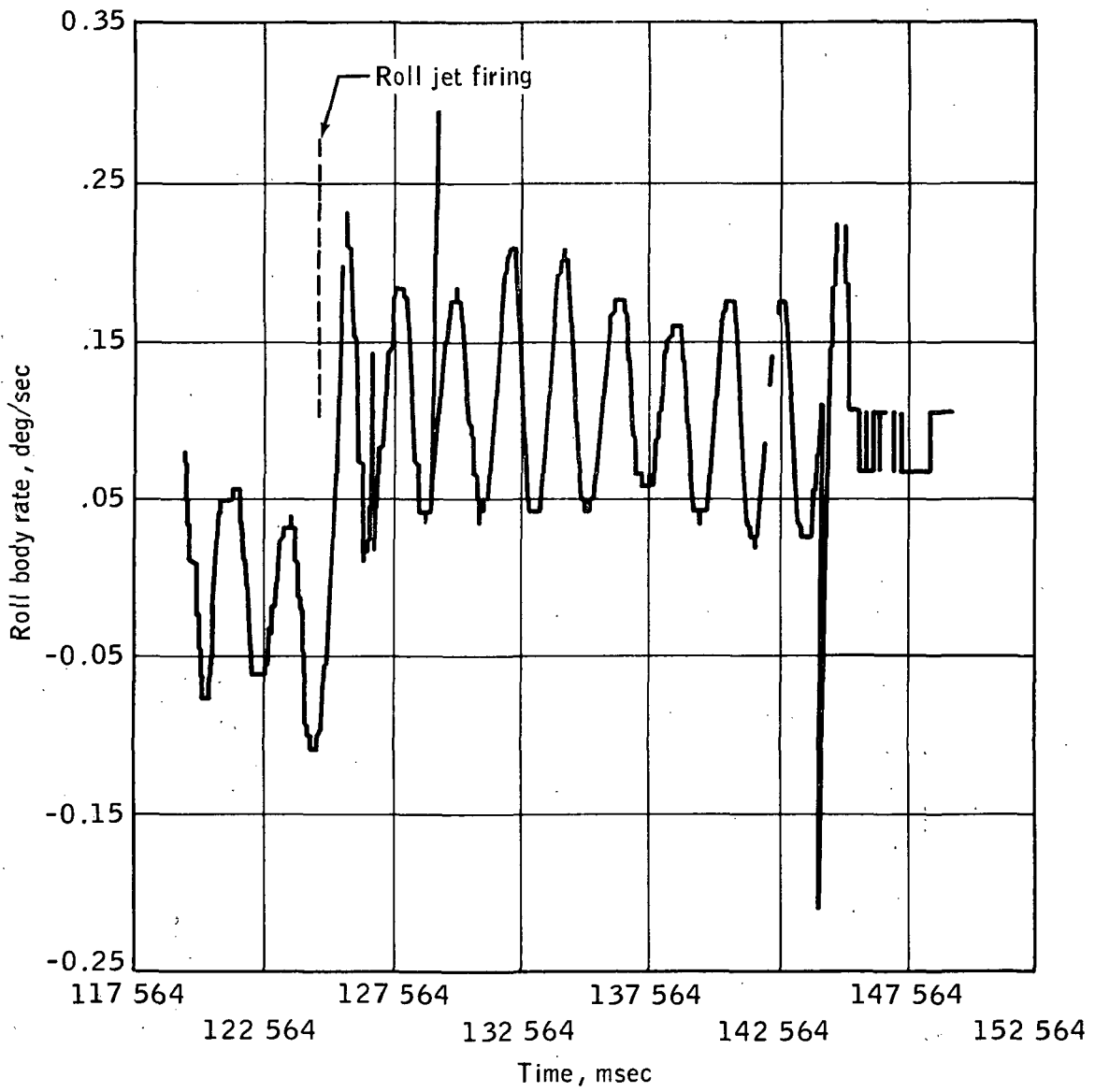


Figure 10. - Time response for the roll body rates.

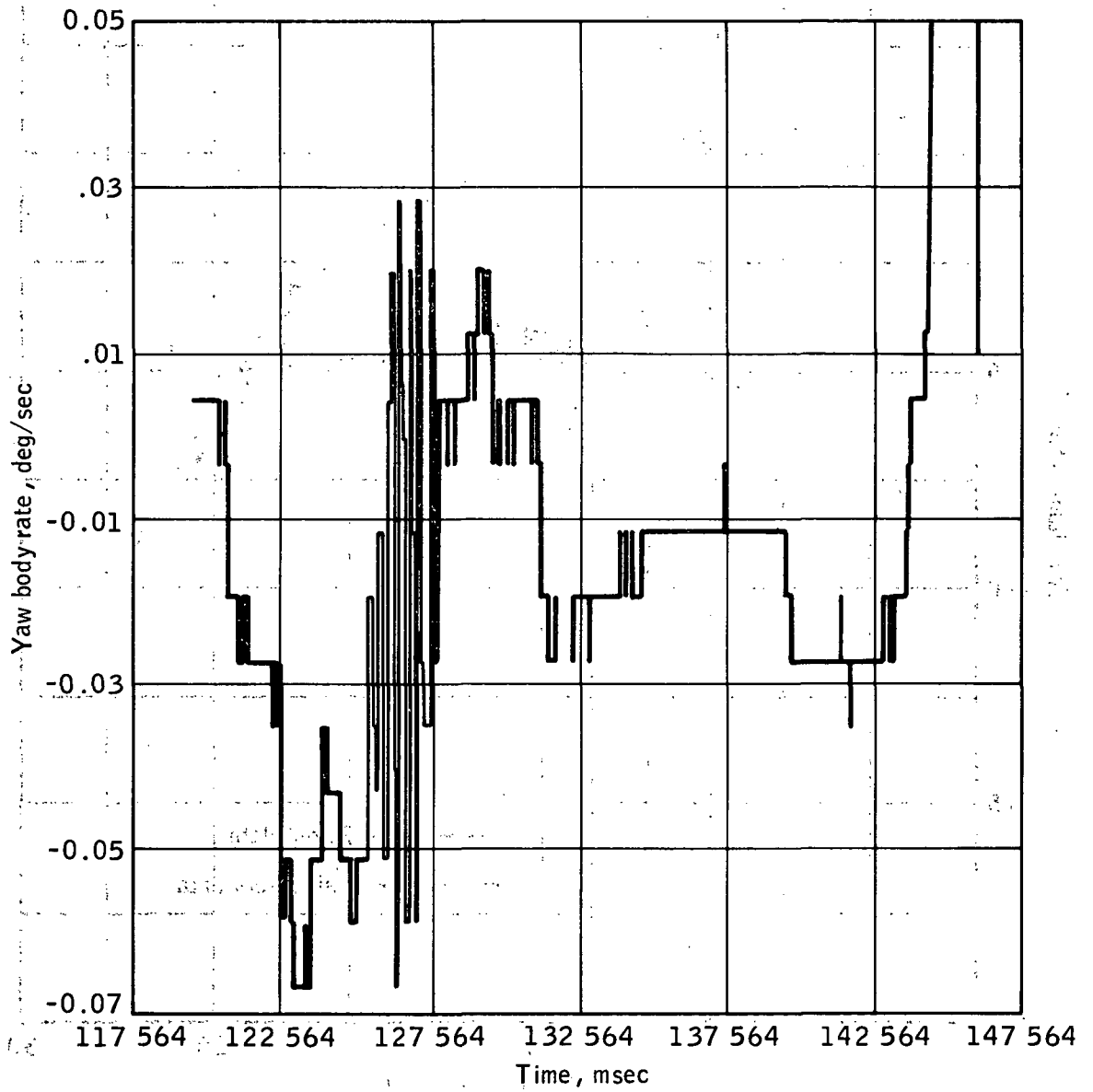
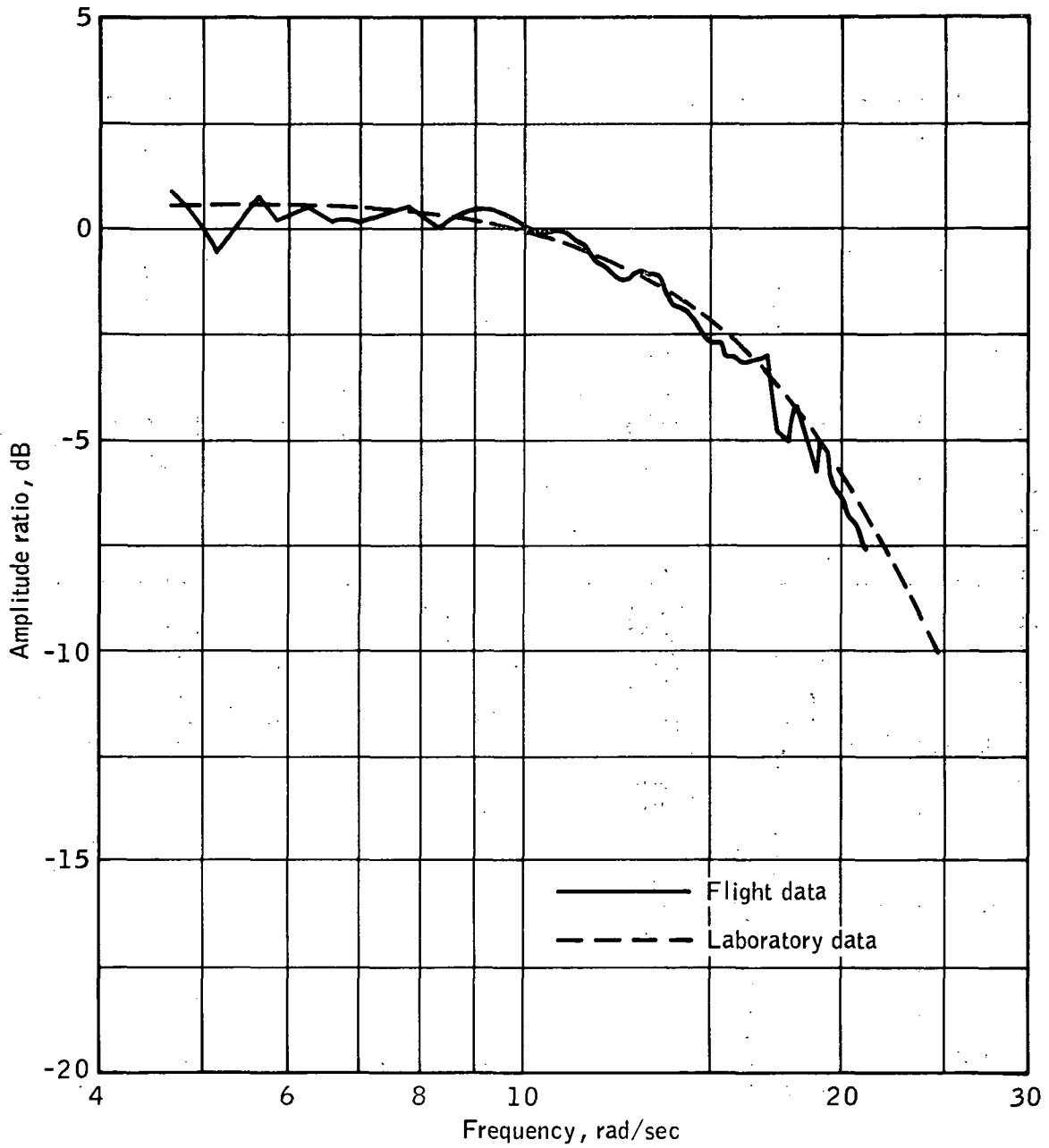
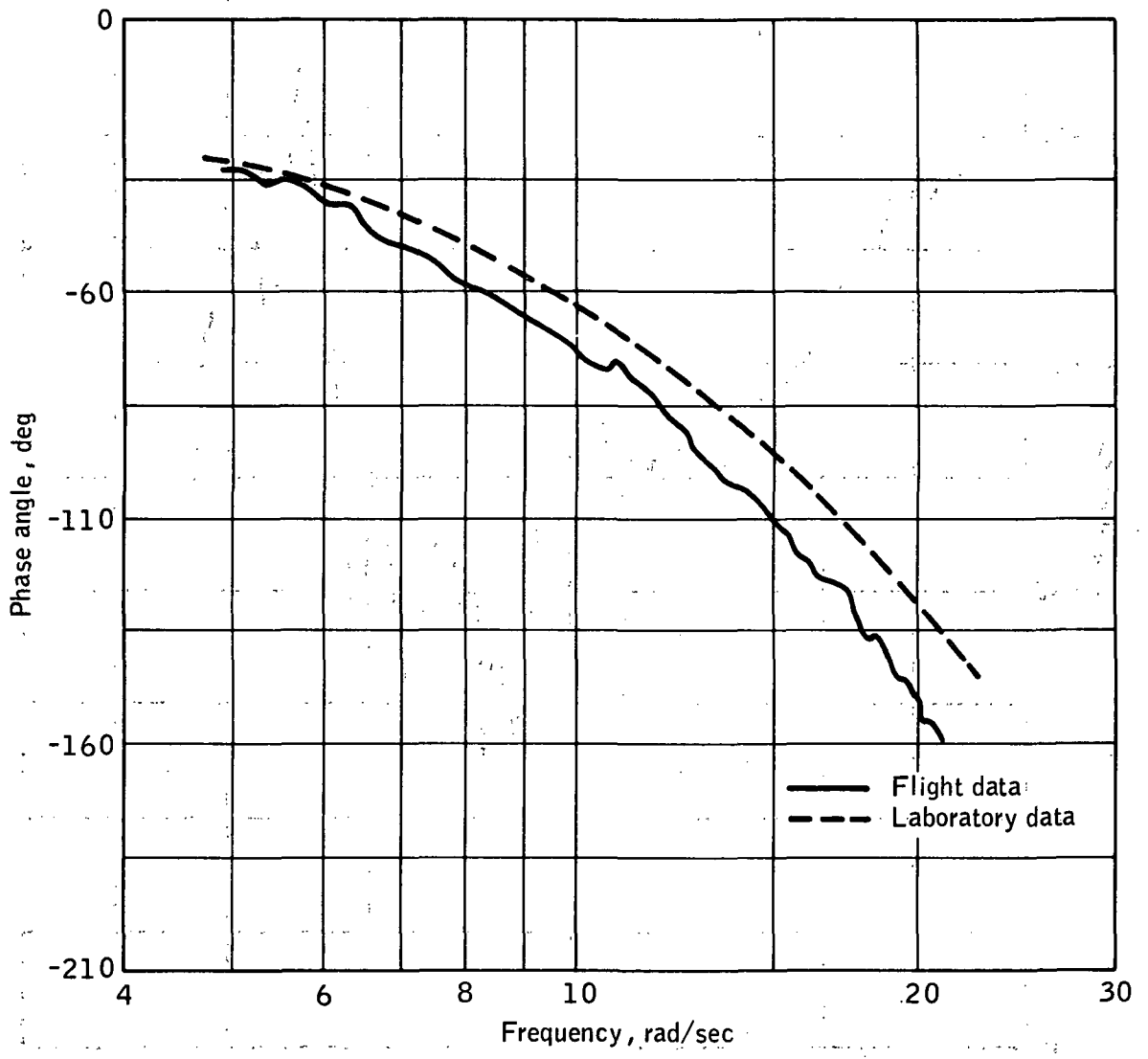


Figure 11. - Time response for the yaw body rates.



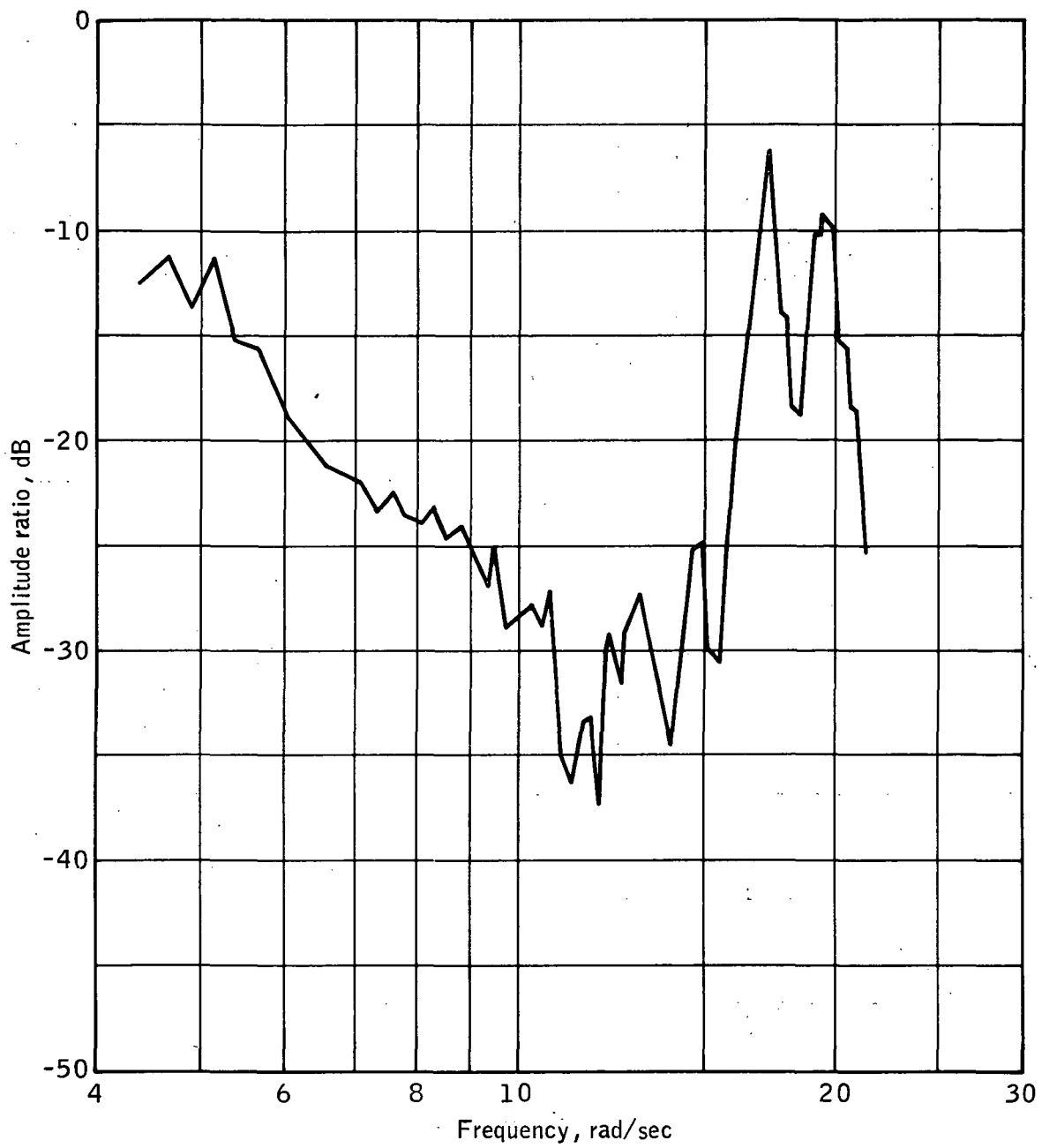
(a) Amplitude ratio.

Figure 12. - Frequency response for the SPS engine pitch actuator.



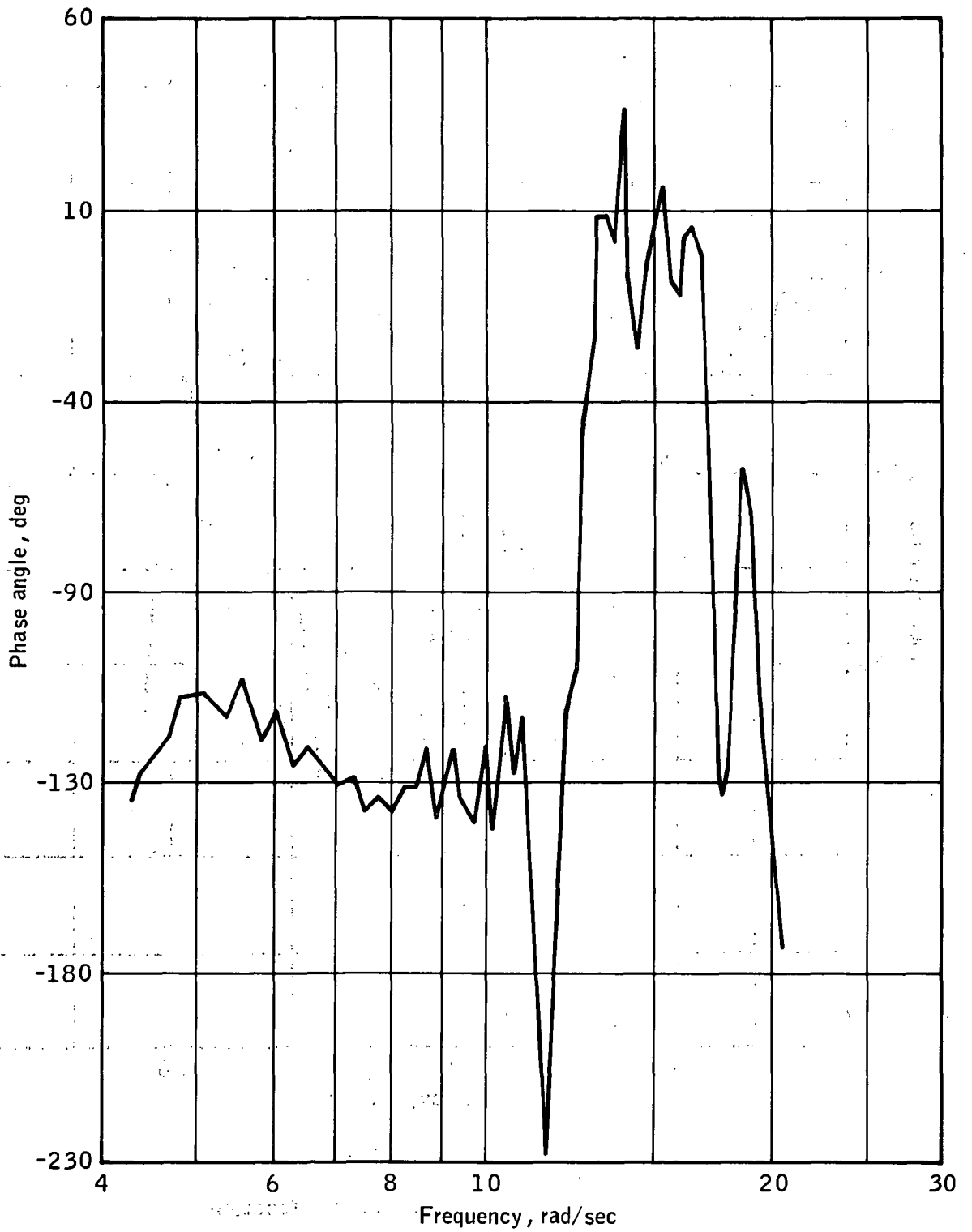
(b) Phase angle.

Figure 12. - Concluded.



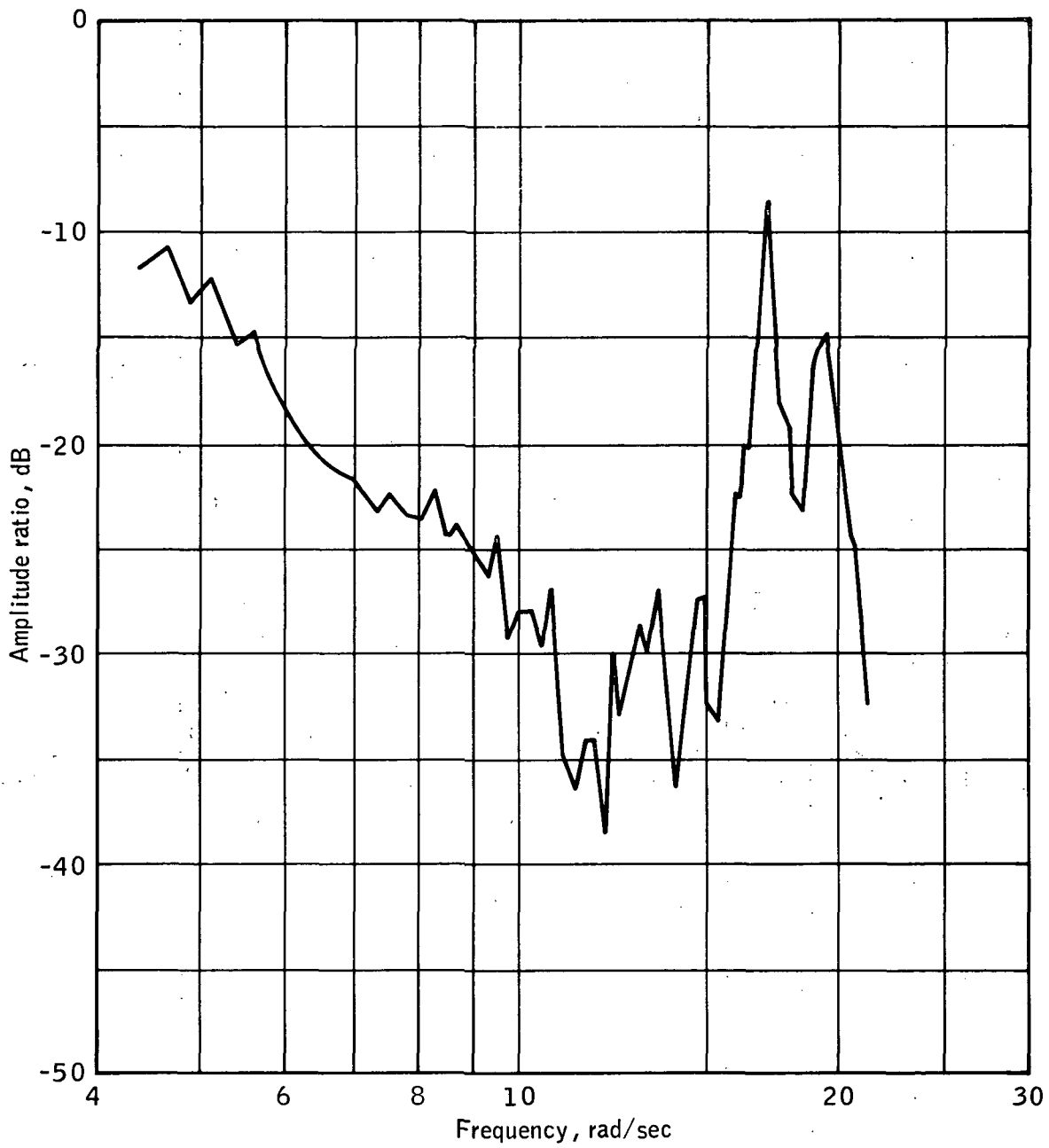
(a) Amplitude ratio.

Figure 13. - Postflight airframe transfer function.



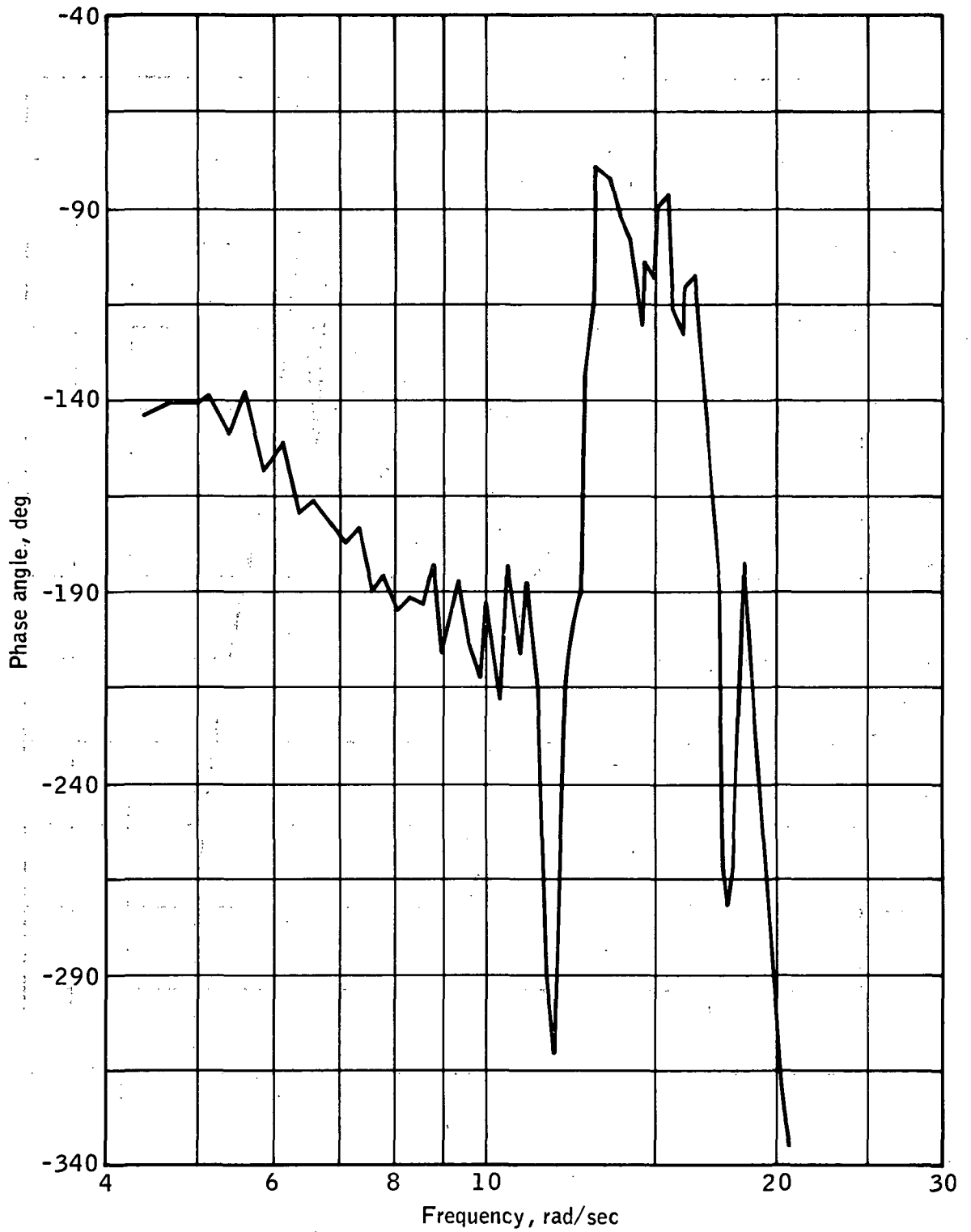
(b) Phase angle.

Figure 13. - Concluded.



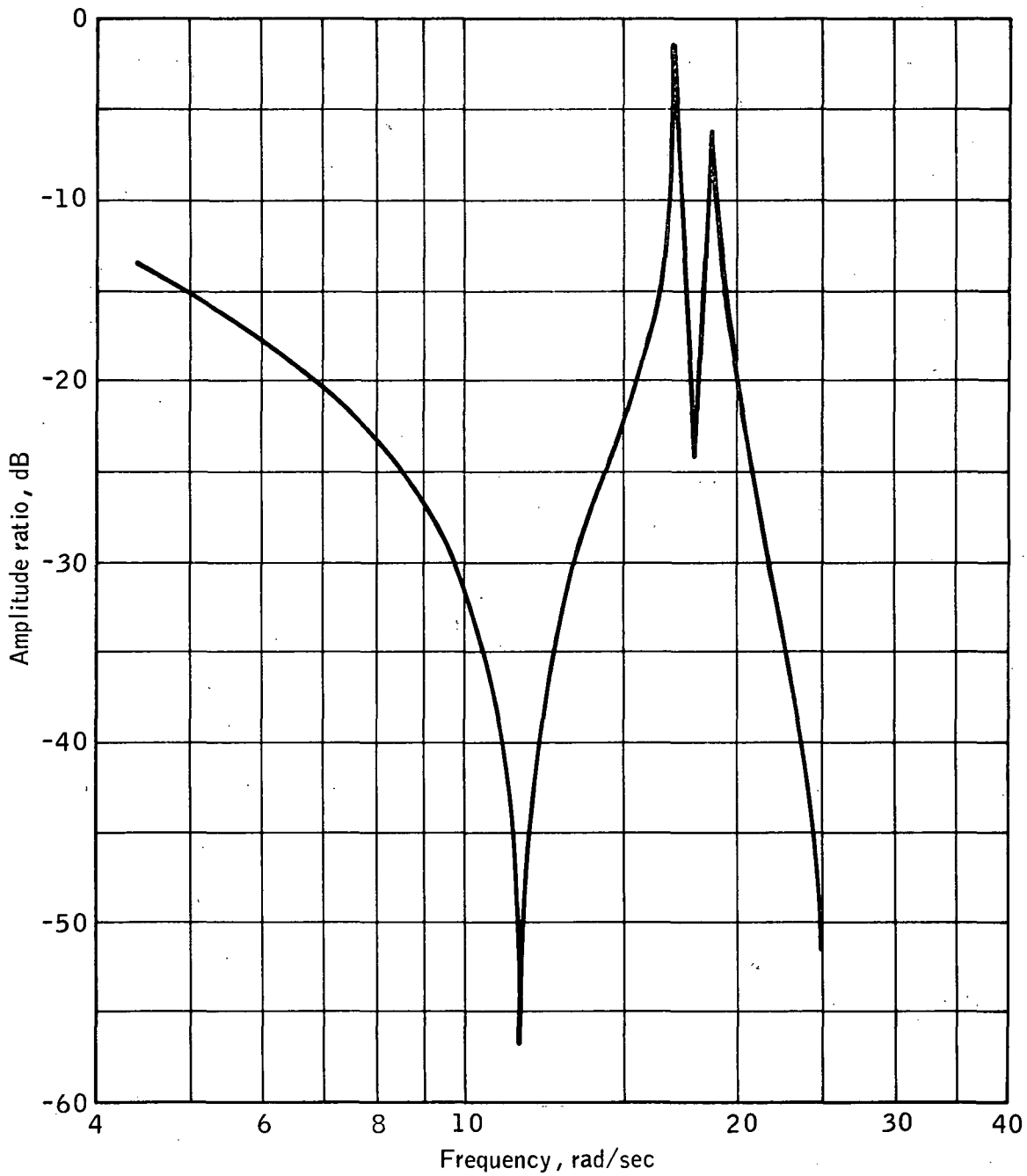
(a) Amplitude ratio.

Figure 14. - Total-system transfer function.



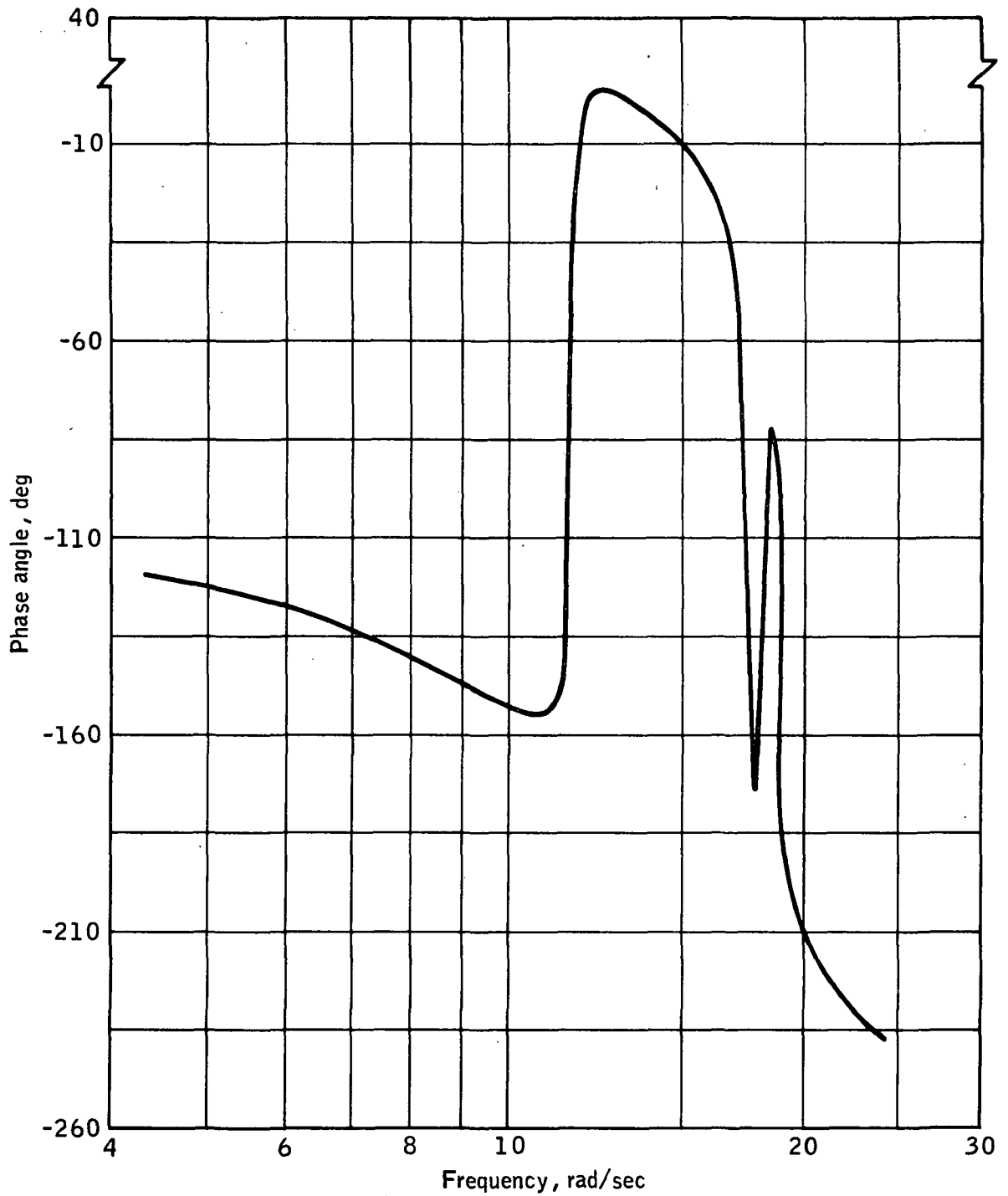
(b) Phase angle.

Figure 14. - Concluded.



(a) Amplitude ratio.

Figure 15. - Preflight total-system transfer function.



(b) Phase angle.

Figure 15. - Concluded.

NASA — MSC